metals

MDPI

Article

Effect of Damage Rate on the Cavity Swelling of Pure Nickel Irradiated with Triple Ion Beams

Jia Huang [1], Zhiying Gao [1], Haocheng Liu [2], Pengfei Ma [3], Yan Liu [3], Wei Ge [1], Fengping Luo [1], Liuxuan Cao [3], Jinchi Huang [3], Jianming Xue [1], Yugang Wang [1] and Chenxu Wang [1,*]

[1] State Key Laboratory of Nuclear Physics and Technology, Center for Applied Physics and Technology, Peking University, Beijing 100871, China; jiahuang@pku.edu.cn (J.H.); zhiyinggao@pku.edu.cn (Z.G.); gewei@pku.edu.cn (W.G.); lfp@stu.pku.edu.cn (F.L.); jmxue@pku.edu.cn (J.X.); ygwang@pku.edu.cn (Y.W.)
[2] State Power Investment Corporation Research Institute, Beijing 102209, China; liuhaocheng@spic.com.cn
[3] College of Energy, Xiamen University, Xiamen 361102, China; 32420191152349@stu.xmu.edu.cn (P.M.); liuyan3579@126.com (Y.L.); caoliuxuan@xmu.edu.cn (L.C.); huangjinchi@xmu.edu.cn (J.H.)
* Correspondence: cxwang@pku.edu.cn

Abstract: He-H synergistic effects influence the performance of structural materials in fusion reactors. Due to the lack of high-intensity fusion neutron sources, multiple ion beam irradiation has been widely used as an emulation method to study its synergistic effects. However, the damage rate under multiple ion beam irradiation is three to four orders of magnitude higher than that under fusion neutron irradiation, and its effect on the cavity swelling is still unclear. In this study, pure nickel was irradiated with single and triple ion beams to ~1 displacements per atom (dpa) at 450 °C. The damage rate ranged from 1.4×10^{-4} to 1.4×10^{-3} dpa/s, with the identical gas-dose ratios of ~400 H appm/dpa and 100 He appm/dpa. Large and isolated cavities formed under single ion irradiation, while triple ion irradiation induced smaller and denser cavities and higher swelling. As the damage rate increased, the cavity size, density, and swelling decreased, due to the constraint of cavity nucleation and growth processes. The effect of damage rate on cavity evolution under triple ion irradiation strongly depends on two competing factors: the enhancement of aggregation and binding of H/He/vacancies, and the enhancement of vacancies–interstitials recombination with increasing damage rate.

Keywords: damage rate; triple ion beam irradiation; He-H synergistic effect; cavity; swelling

check for updates

Citation: Huang, J.; Gao, Z.; Liu, H.; Ma, P.; Liu, Y.; Ge, W.; Luo, F.; Cao, L.; Huang, J.; Xue, J.; et al. Effect of Damage Rate on the Cavity Swelling of Pure Nickel Irradiated with Triple Ion Beams. *Metals* **2022**, *12*, 1106. https://doi.org/10.3390/met12071106

Academic Editor: Cemal Basaran

Received: 31 May 2022
Accepted: 25 June 2022
Published: 28 June 2022

Publisher's Note: MDPI stays neutral with regard to jurisdictional claims in published maps and institutional affiliations.

Copyright: © 2022 by the authors. Licensee MDPI, Basel, Switzerland. This article is an open access article distributed under the terms and conditions of the Creative Commons Attribution (CC BY) license (https://creativecommons.org/licenses/by/4.0/).

1. Introduction

The development of commercial magnetic confinement fusion energy is accelerating, while the tolerance of structural materials exposed to high temperatures and intense radiation fields remains a major challenge. During the operation of structural materials, one critical form of structural damage is the volumetric swelling induced by cavity formation through vacancies aggregation and evolution. The swelling typically occurs in the temperature range of 0.3 to 0.6 T_M (melting temperature), resulting in detrimental volumetric expansion, mechanical strength degradation, and even rupture of structural materials, which then severely threatens the integrity and safety of reactors [1].

In fusion reactors, the D-T reaction produces 14 MeV high-energy neutrons, resulting in a much harder neutron energy spectrum than that in a commercial fission reactor. High-energy fusion neutrons produce high-level displacement damage in structural materials, and simultaneous production of large amounts of hydrogen (H) and helium (He) atoms through (n, α) and (n, p) transmutation reactions [2]. These gas atoms have synergistic effects with displacement defects, significantly influencing cavity behaviors in structural materials, aggravating irradiation swelling, and accelerating the degradation of the materials in operation [3].

The resistance of structural material to fusion neutron irradiation needs to be fully evaluated prior to application in fusion reactors. However, up to now, there have been no available high-intensity fusion neutron sources. Limited experimental data have described the microstructural evolution induced by fusion neutron irradiation at very low doses [4,5]. Currently, the development and evaluation of candidate materials mostly rely on fission neutron and spallation neutron irradiation. However, the radiation effects induced by fission and spallation neutrons significantly differ from those caused by fusion neutrons, due to the substantial differences in the production rate of transmutated H and He [2,6,7]. This requires other experimental emulation methods that could produce equivalent concentrations of H and He with displacement defects in materials to those under fusion neutron irradiation.

Multiple simultaneous ion beam irradiation (MSIB), which integrates two or three beamlines of heavy ions, H ions, and He ions, is attracting increasing attention. Its primary advantage is that the gas–dose ratio in the irradiated materials can be controlled, which is of great help in investigating the He–H synergistic effects. Compared to neutron irradiation, MSIB irradiation can accumulate high levels of displacement doses, helium and hydrogen in a relatively short period of time with almost no residual radioactivity. Additionally, the key irradiation parameters (temperature, dose, H and He concentrations, etc.) can be systematically controlled.

However, accumulation of high doses in such a short period of time leads to the inevitable disadvantage that the displacement–production rate is too high. In MSIB, in addition to the displacement–production rate (dpa/s), the gas implantation rate of H and He (appm/s) also plays an important role in the irradiation effect, and these are collectively referred to as the damage rate. Although the damage rate in MSIB irradiation can be controlled within a certain range, it is still three to four orders of magnitude higher than that of fusion neutron irradiation. This difference in damage rate can result in dramatically different irradiation effects [8,9]. Under neutron irradiation, relatively uniform and dispersed displacement cascades are formed, whereas the cascades are significantly denser due to the higher nuclear stopping power and higher fluxes under heavy ion irradiation [10]. Therefore, it is generally expected that with increasing displacement–production rate the recombination of vacancies and self-interstitial atoms will be enhanced and the swelling will be reduced [11,12].

In MSIB irradiation, implanted He and H combine with vacancies to form vacancy–gas clusters, which may act as cavity nucleation embryos [13]. The synergistic binding between H, He, and the vacancies directly affects the three main behaviors of vacancies, i.e., recombination with interstitials, aggregation into voids, and escape into free defects [10,14]. Therefore, the evolution of vacancies under MSIB irradiation is more complicated than under single ion irradiation. However, there is little understanding of the complicated effects of damage rate on vacancy and cavity evolution when H and He gas atoms exist simultaneously.

MSIB irradiation has been used for many years to study the He–H synergistic effects on cavity behavior and the swelling of materials. Many results have shown that swelling was significantly enhanced, even up to a hundred times [15,16]. These results raised concerns about the performance of materials in the fusion reactor environment, however, they were also questioned due to the high damage rates of MSIB experiments. There is also a discrepancy regarding the specific effects of H and He on cavity behaviors, which may be related to differences in irradiation temperatures, material systems, damage rates, etc. [17]. However, the effects of damage rate in MSIB irradiation have not often been reported, especially when both H and He are present. Taller and Was [18] investigated the effect of damage rate on cavity behaviors in T91 at a fixed He–dose ratio under (Fe + He) dual ion irradiation. They found that an increase in damage rate slightly reduced cavity nucleation, which was confirmed by simulation results [19,20], but no significant influence was observed and no clear conclusions were obtained.

In this work, the effects of damage rate on cavity behavior and swelling in pure nickel under single and triple ion beam irradiation are investigated. Nickel was selected to allow a comparison with the swelling results induced by fusion neutron irradiation [21]. The pure metal benchmark system facilitated the acquisition of general laws by minimizing the potential influence of alloying elements and initial microstructures [22]. Our results show that a high damage rate reduced cavity size, density, and swelling. However, the introduction of H and He under triple ion irradiation weakened this effect due to the competition between the simultaneous enhancement of synergistic binding of H/He/vacancies and vacancy–interstitial recombination. This study contributes a deeper understanding of MSIB irradiation in studying the He–H synergistic effects.

2. Materials and Methods

Polycrystalline nickel with a purity of more than 99.99% was used in this study. Disk-shaped samples with a diameter of 3 mm were cut by Electric Discharge Machining (EDM), followed by vacuum annealing at 800 °C for 2 h. Then, the samples were mechanically ground to 100 μm step by step using SiC abrasive papers and polished to a mirror-like surface using 0.05 μm colloidal silica suspension, prior to irradiation.

Irradiation was performed in the Xiamen Multiple Ion Beam In-situ TEM Analysis Facility (Xiamen University, Xiamen, China) [23]. The disk sample was mounted onto a heater specimen holder (Gatan 652) inside the TEM specimen chamber, and the irradiation temperature was maintained at 450 °C. The defocused 400 keV Ni^+ and 50 keV He^+ and H_2^+ beams were at an angle of 20° and 25° to the sample normal, respectively. The two beams were at an angle of 45° to each other, as shown in Figure 1a. The damage profile and concentrations of He and H under the set irradiation conditions were calculated using SRIM-2013 with the Quick K-P option, as shown in Figure 1b. In the calculation, the 50 keV H_2^+ was treated as two 25 keV H atoms [24]. The displacement threshold energy and the lattice binding energy were set to 40 eV and 0 eV, respectively [25]. To minimize the possible interference of surface effects, a depth of 100-250 nm below the surface was set as the examination region [26]. For comparison, (Ni+H+He) triple ion irradiation and single Ni ion irradiation were each performed at 450 °C. The dose rates (displacement–production rate) were set to 1.4×10^{-4}, 4.6×10^{-4}, and 1.4×10^{-3} dpa/s, averaged over the examination region, corresponding to irradiation times of 8450 s, 2755 s, and 845 s, respectively. Meanwhile, the gas–dose ratios were fixed at about 400 H appm/dpa and 100 He appm/dpa, respectively. The total amount of accumulative dose and gas was ~1 dpa, ~400 appm H, and ~100 appm He over the examination region. The displacement dose induced by He and H was less than 0.001% and thus could be neglected. Following the triple ion irradiation, dose rates of 1.4×10^{-4}, 4.6×10^{-4}, and 1.4×10^{-3} dpa/s were used to represent the damage rates, including the displacement–production rates and the corresponding gas implantation rates.

This study mainly focused on the effect of damage rate under single and triple ion irradiation observed through relative comparison, and was not intended to provide generic absolute values of irradiation cavity and swelling. Thus, the effects of free surfaces and injected ions on the behaviors of vacancy and H and He, although they cannot be completely avoided due to the limitation of penetration depth, could be uniformly treated as extra defect sinks under both irradiation types. The fluctuations in dose and concentrations of H and He over the examination region were considered in the same way. In the relative comparison of single and triple ion irradiation, the interference of the treatment in the discussion of damage rate effects was minimal.

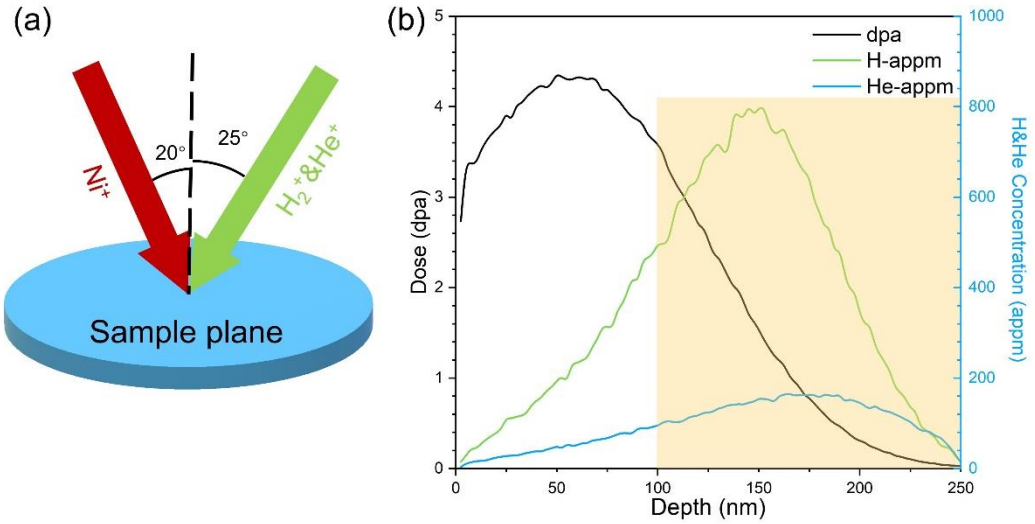


Figure 1. (**a**) Schematic diagram of the geometric relationship between sample and beamlines; (**b**) The SRIM profiles of displacement damage (left axis) and gas concentration (right axis) in pure nickel under MSIB irradiation. The triple ion beams included 400 keV Ni^+ and 50 keV He^+ & H_2^+. The orange box represents the examination region at a depth of 100–250 nm below the surface, where average accumulative dose and gas concentration was ~1 dpa, ~400 appm H and ~100 appm He.

This study focused on cavity swelling, i.e., the expansion of materials volume, which can be calculated as the total volume of all cavities in a selected area divided by the volume of the matrix in this area [16]. Cross-section TEM specimens after irradiation were prepared using focused-ion beam (FIB) with a standard "lift-out" procedure [27] on a Helios G4 UX (FEI Company, Hillsboro, OR, USA). Post-irradiation microstructures were characterized using a Tecnai F20 (FEI Company, Hillsboro, OR, USA) transmission electron microscope (TEM). For each irradiation condition, bright-field TEM images were taken at defocus and over-focus of about 800 nm with an objective diaphragm, to identify possible cavities. Then, the size and density of the cavities were measured manually using ImageJ software (v1.52a, National Institutes of Health, USA) to calculate their volume. More than 400 cavities in several randomly selected regions under triple ion beam irradiation were counted for each damage rate. The thickness of each specimen was determined by electron energy loss spectrometry (EELS), ranging from 60 to 90 nm. Errors in manual measurements (5%), random errors in counting ($\sqrt{N}$), and errors in EELS measurement (10%) were considered in the calculations.

3. Results

Figure 2 shows the defocused TEM images of samples with various damage rates after single and triple ion beam irradiation to ~1 dpa. Cavities with considerably different distributions were observed under all irradiation conditions. After Ni^+ ion irradiation, isolated and relatively large cavities formed in the materials, as shown in Figure 2a–c. These cavities were mainly distributed at the depth of 100–200 nm below the surface. As the dose rate increased, the size of the cavity decreased, indicating the effect of the dose rate on cavity growth. In contrast, the morphology of cavities after triple ion beam irradiation differed from that after single Ni ion beam irradiation, as shown in Figure 2d–f. Figure 2g–i are the enlarged images of Figure 2d–f, respectively. Smaller cavities with higher density were observed at depths of 100–250 nm, as indicated by the yellow arrows. As the damage rate increased, the cavity size decreased slightly, as shown in Figure 2g–i. These obvious differences in size and density of cavities after single and triple ion beam irradiation reveals the synergistic effects of H, He, and vacancies on cavity nucleation and dispersion.

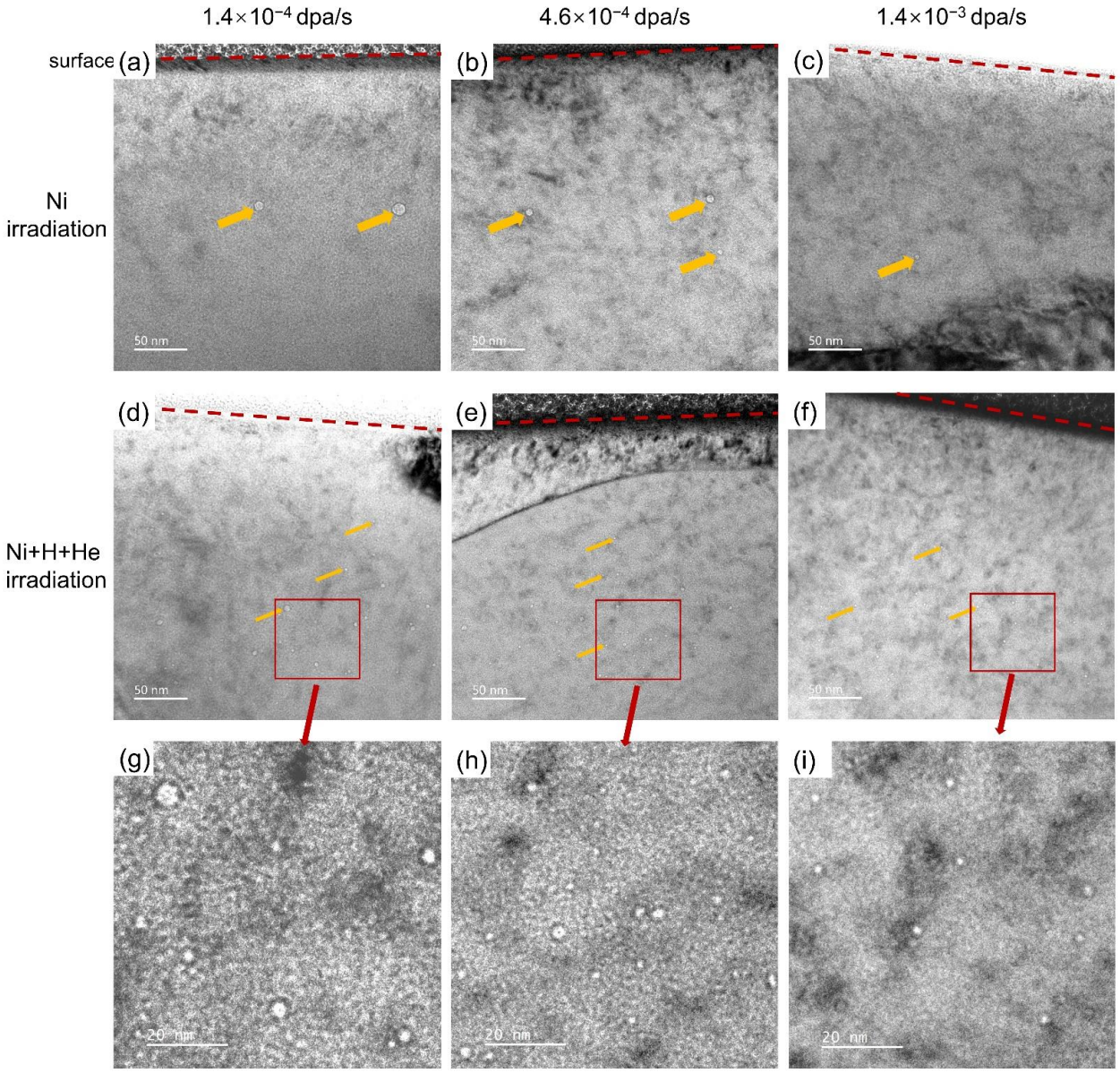


Figure 2. Bright field TEM images of cavities in pure nickel induced by (**a**–**c**) Ni^+ irradiation and (**d**–**f**) (Ni+H+He) triple ion irradiation at 450 °C to ~1 dpa. (**a**,**d**), (**b**,**e**), (**c**,**f**) correspond to the damage rate of 1.4×10^{-4}, 4.6×10^{-4} and 1.4×10^{-3} dpa/s, respectively. A few typical cavity examples are indicated by yellow arrows. The red dashed lines indicate the specimen surface. (**g**–**i**) are local zoomed images of the red boxed areas in (**d**–**f**), as indicated by the arrows.

Based on the TEM results shown in Figure 2, the cavity size and number densities after single and triple ion beam irradiation were analyzed, respectively, as shown in Figure 3a,b. The Ni^+ ion irradiation produced cavities with average diameters larger than 4.5 nm at all three dose rates. The average diameters were 7.9 ± 2.9 nm, 6.0 ± 2.2 nm, and 4.7 ± 0.9 nm at dose rates of 1.4×10^{-4}, 4.6×10^{-4}, and 1.4×10^{-3} dpa/s, respectively. This indicates the gradual decrease of average size with increasing dose rate. The specific size distributions of the cavities also differed, as shown in Figure 4a. As the dose rate decreased, the distribution gradually broadened, and the average size increased. The cavity densities in the samples irradiated by Ni+ irradiation at1.4×10^{-4} dpa/s and 4.6×10^{-4} dpa/s were both around 7×10^{20} m^{-3}, and it greatly decreased to 7×10^{19} m^{-3} as the dose rate increased to 1.4×10^{-3} dpa/s. This indicates the possible constraint effect on cavity nucleation of increasing dose rate. Since the volume of the cavity is proportional to the third power of

the diameter, the larger cavities contributed to a higher swelling. The combination of size and density changes resulted in a gradual decrease in swelling with the increasing dose rate, as shown in Figure 3c. The swelling reached 0.026% under Ni+ irradiation to ~1 dpa at 1.4×10^{-4} dpa/s, and decreased to 0.012% at 4.6×10^{-4} dpa/s. At the highest dose rate, the swelling was only 0.00046%, which can be ignored; the swelling level was so low that it might be more sensitive to certain random or statistical errors.

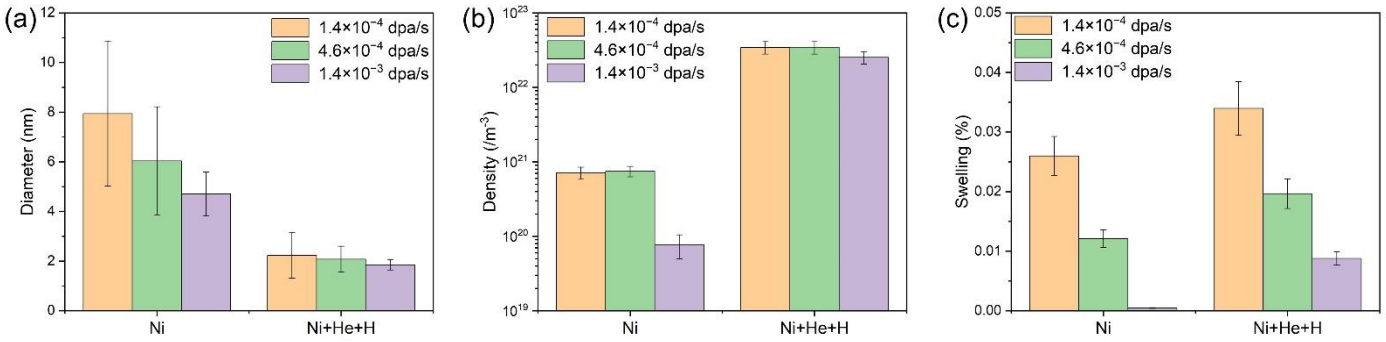


Figure 3. The statistical results of (**a**) cavity average size, (**b**) number density, and (**c**) volume swelling. The *x*-axis shows the irradiation types of single Ni and triple (Ni+H+He) ions. In (**a**–**c**), the orange, green, and purple correspond to the dose rates of 1.4×10^{-4} dpa/s, 4.6×10^{-4} dpa/s, and 1.4×10^{-3} dpa/s, respectively.

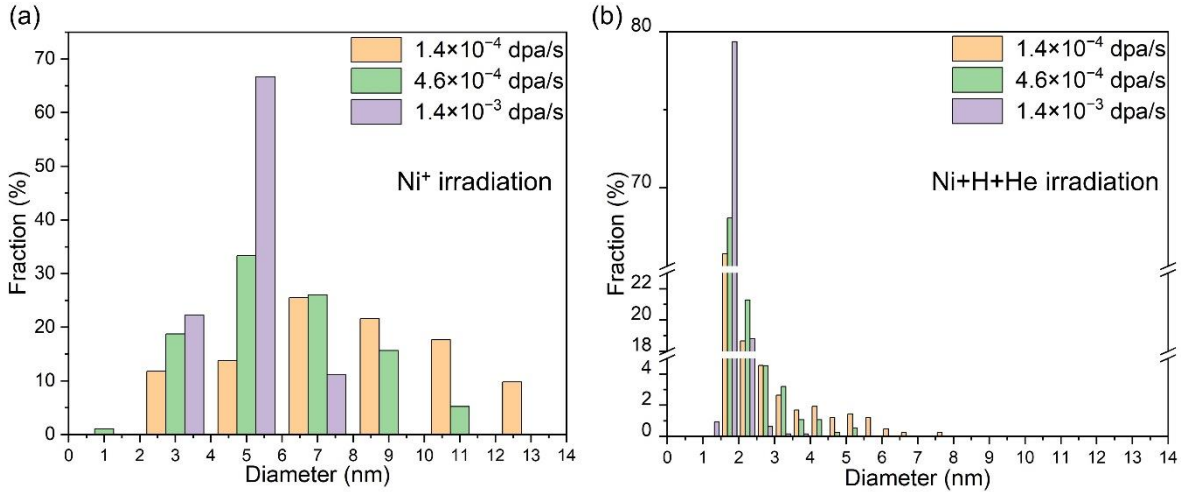


Figure 4. The size distribution of cavities after Ni single ion (**a**) and (Ni+H+He) triple ion irradiation (**b**). The orange, green, and purple correspond to the dose rates of 1.4×10^{-4} dpa/s, 4.6×10^{-4}, and 1.4×10^{-3} dpa/s, respectively. In panel (**b**), two breakpoints at 5–18 and 23–65 are set in the *y*-axis for clarity.

The trends under triple ion beam irradiation were similar; at 1.4×10^{-4} dpa/s, there were cavities of varying sizes of ~2 to 8 nm, whereas only uniform cavities of ~2 nm existed at 1.4×10^{-3} dpa/s, as shown in Figure 4b, and the average size decreased from 2.2 ± 0.9 nm to 1.8 ± 0.2 nm. The cavity densities were 3.4×10^{22} m^{-3}, 3.4×10^{22} m^{-3}, and 2.5×10^{22} m^{-3} at damage rates of 1.4×10^{-4} dpa/s, 4.6×10^{-4} dpa/s, and 1.4×10^{-3} dpa/s, respectively, again showing a clear decrease at the highest damage rate. As a result, the swelling showed a tendency to decrease with increasing damage rate, as shown in Figure 3c. The maximum swelling is 0.034% at 1.4×10^{-4} dpa/s, which was the maximum under all irradiation conditions. When the damage rate increased to 1.4×10^{-3} dpa/s, the swelling reduced to 0.0087%.

4. Discussion

Variation of the damage rate significantly influenced cavity behaviors under both single Ni and triple (Ni+H+He) ion beam irradiation. Since the displacement doses induced by H and He are limited, principal consideration was given to the displacement induced by heavy ions. Cavity formation and growth were mainly dependent on the vacancies that survived the initial cascade stage of irradiation damage. The average free path of heavy ions in materials is much shorter than is the case under neutron irradiation, producing a series of displacement cascades along the trajectory through dense and strong Coulomb elastic collisions. Within these cascades and between the nearby cascades, most produced vacancies and interstitials recombine at ~10^{-11} s, and only a small fraction can escape becoming free point defects or self-aggregating into clusters [28,29]. In this work, we adjusted the ion beam current, i.e., ion fluxes (ions·cm^{-2}·s^{-1}), to change the damage rate. Thus, as the Ni-ion flux increased in the single ion irradiation, the spatial distances between different heavy ion trajectories and their cascades were even closer. The denser cascades would enhance the recombination and annihilation of point defects, reducing the steady-state vacancy concentration (Cv) and the density of the aggregation–vacancy clusters (the recombination–dominant case considered herein annealed pure nickel) [30]. The smaller C_v at a higher dose rate would directly reduce the cavity growth rate, according to the rate theory for cavity growth [10,31]. Meanwhile, the vacancy clusters acted as the original cavity nucleation sites, such that the cavity nucleation process weakened with the increasing dose rate. In our single ion irradiation experiment, with increasing dose rate, the reduced nucleation and growth processes together led to the decrease in cavity density, size, and swelling, as shown in Figure 3.

H and He also induced pronounced synergistic effects in the samples under triple ion irradiation. Previous studies have reported the inhibition of vacancies–interstitials recombination by He [32] and H [33] alone. During triple ion irradiation, H, He, and displacement cascades induced by heavy ions coexist in a relatively small region. Vacancies and interstitials that survive from cascades are randomly located in this region. H and He are likely to be captured by the adjacent vacancies, forming He-H-V clusters. This synergistic binding effectively inhibits the direct recombination of vacancies with interstitials, subsequently reducing the mobility of vacancies and stabilizing small vacancy clusters [34,35]. Thus, the cavity nucleation site increases, enhancing the nucleation and dispersion of cavities. This explains our experimental results showing that the introduction of H and He led to much higher cavity density and higher swelling in samples irradiated at the same displacement–production rate, as shown in Figure 3b,c, even when the vacancies–interstitials recombination was considerably enhanced as the displacement–production rate increased.

Based on the above discussion, we believed that the evolution of cavities with increasing damage rates under triple ion irradiation strongly depends on two competing factors. One is the enhancement of aggregation and binding between H/He and vacancies, and the other is the enhancement of vacancies–interstitials recombination. Since the gas–dose ratio (appm/dpa) was essentially identical at different dose rates, the implantation rates (appm/s) of H and He varied simultaneously with the displacement–production rates. As the damage rate increased, the concentrations of H, He, and vacancies coexisting in the same region increased, leading to a higher probability of H and He being captured and the formation of He-H-V clusters. As a result, the number of surviving vacancies and the cavity nucleation sites increased, promoting the nucleation and growth process of the cavity. However, as discussed earlier, the enhancement of vacancies–interstitials recombination due to increasing damage rate led to a decrease in the steady-state vacancy concentration C_v and the cavity nucleation sites. Under triple ion irradiation conditions, as shown in Figure 3, the cavity size, density, and swelling decreased with increasing damage rate, indicating that the enhancement of the recombination process dominated in this competition. Nevertheless, the enhancement of the aggregation and binding process of H, He, and vacancies still weakened the enhancement effect of recombination in samples irradiated at

high damage rates. This is confirmed by our results, as shown in Figure 3, indicating that the reduction of cavity average size and density with increasing damage rate after triple ion irradiation was much less than after single Ni ion irradiation. Since the environments (temperature, dose, dose rate, and H/He concentration) and the microstructures (grain size, composition, lattice structure, and precipitation) are expected to influence this competing process, the dominant factor in the competition and the experimental phenomena may be different under other experimental conditions. Therefore, further investigation is needed to determine the quantitative contribution of the enhanced synergistic effect and enhanced recombination at high damage rates.

The concern about the damage rate issue stems mainly from the emulation of neutron irradiation effects via ion irradiation. The data obtained from this study were compared with the only available fusion neutron irradiation data [21] for pure nickel samples at the same temperature, as shown in Figure 5. The fission neutron irradiation data at similar doses and the same temperatures are plotted for comparison [36]. It has been reported that the irradiation swelling induced by fusion neutron irradiation was significantly larger than that after fission neutron, indicating the roles of transmuted H and He in cavity evolution [37]. As shown in Figure 5, fusion neutron irradiation at dose rates of 10^{-8} dpa/s induced higher swelling than seen with triple ion irradiation in the present work, even though their doses were much lower. This suggests that the swelling induced from synergistic effects also increased with decreasing damage rate varying over five orders of magnitude, which is in agreement with the tendency observed in multiple ion beam irradiation experiments in this study.

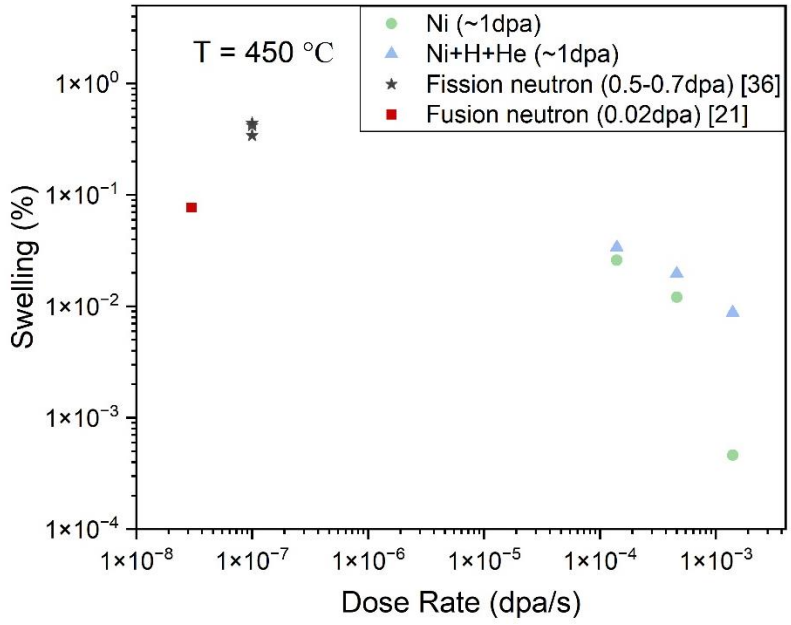


Figure 5. Comparison of data from this work with data of pure nickel irradiated by fusion neutron (from ref. [21]) and fission neutron (from ref. [36]). The irradiation temperatures were all 450 °C.

5. Conclusions

In this study, single Ni ions and (Ni+H+He) triple ions were used to irradiate pure nickel samples to about ~1 dpa at 450 °C, with damage rates ranging from 1.4×10^{-4} to 1.4×10^{-3} dpa/s and identical gas–dose ratios of ~400 H appm/dpa and 100 He appm/dpa. For the first time, the effects were studied of damage rate on swelling under (heavy ion +H + He) triple ion irradiation. Triple ion irradiation triggered the formation of much denser and smaller cavities and higher swelling than did single ion irradiation, suggesting a synergistic effect between H, He, and vacancies on the promotion of cavity nucleation and dispersion. For both irradiation types, the increase in damage rate generally led to a decrease

in the density and size of cavities, indicating the enhancement effects of damage rate on the vacancies–interstitials recombination process. These results, together with the neutron irradiation data, suggest that irradiation swelling generally increases with decreasing damage rate. When both H and He were present, the reduction in cavity size, density, and swelling caused by increasing damage rate was much less than under single Ni ion irradiation, indicating the competition between the enhanced synergistic binding of H/He/vacancies and the enhanced vacancies–interstitials recombination at higher damage rates. Considering the complex influence of numerous experimental parameters (temperature, dose, dose rate, gas concentration, and material system) and the relatively narrow range of damage rate covered in this work, quantitative conclusions could not be obtained concerning the effects of damage rate under triple ion beam irradiation. However, by relative comparison, this study provides qualitative insight into the effects of damage rate on cavity swelling resulting from the He-H synergistic effects under fusion neutron irradiation. In the future, systematic experiments are needed across a wide range of damage rates (more than two orders of magnitude) and various parameters involving a selection of materials, to enhance our understanding of the effects of multi-ion beam irradiation on fusion neutron irradiation.

Author Contributions: Conceptualization, C.W., J.X. and Y.W.; formal analysis, J.H. (Jia Huang), W.G. and F.L.; investigation, J.H. (Jia Huang), Z.G., H.L., P.M., Y.L. and J.H. (Jinchi Huang); resources, L.C.; writing—original draft preparation, J.H. (Jia Huang); writing—review and editing, Z.G., H.L., C.W., J.X. and Y.W.; funding acquisition, J.X. and Y.W. All authors have read and agreed to the published version of the manuscript.

Funding: This research was funded by the National MCF Energy R&D Program (Grant No. 2022YFE03110000) and the National Natural Science Foundation of China (Grant No. 12192280 and Grant No. 11935004).

Institutional Review Board Statement: Not applicable.

Informed Consent Statement: Not applicable.

Data Availability Statement: The data presented in this study are available in article.

Acknowledgments: The authors acknowledge Electron Microscopy Laboratory of Peking University for the use of TEM and FIB.

Conflicts of Interest: The authors declare no conflict of interest.

References

1. Zinkle, S.J.; Busby, J.T. Structural materials for fission & fusion energy. *Mater. Today* **2009**, *12*, 12–19. [CrossRef]
2. Dai, Y.; Odette, G.; Yamamoto, T. The Effects of Helium in Irradiated Structural Alloys. In *Comprehensive Nuclear Materials*, 2nd ed.; Konings, R., Stoller, R., Eds.; Elsevier: Amsterdam, The Netherlands, 2020; Volume 1, pp. 186–234.
3. Marian, J.; Hoang, T.; Fluss, M.; Hsiung, L.L. A review of helium–hydrogen synergistic effects in radiation damage observed in fusion energy steels and an interaction model to guide future understanding. *J. Nucl. Mater.* **2015**, *462*, 409–421. [CrossRef]
4. Logan, C.M.; Heikkinen, D.W. RTNS-II—A fusion materials research tool. *Nucl. Instrum. Methods Phys. Res.* **1982**, *200*, 105–111. [CrossRef]
5. Kiritani, M.; Yoshida, N.; Ishino, S. The Japanese experimental program on RTNS-II of DT-neutron irradiation of materials. *J. Nucl. Mater.* **1984**, *122*, 602–607. [CrossRef]
6. Muroga, T.; Heinisch, H.L.; Sommer, W.F.; Ferguson, P.D. A comparison of microstructures in copper irradiated with fission, fusion and spallation neutrons. *J. Nucl. Mater.* **1992**, *191–194*, 1150–1154. [CrossRef]
7. Knaster, J. An assessment of the available alternatives for fusion relevant neutron sources. *Nucl. Fusion* **2018**, *58*, 095001. [CrossRef]
8. Was, G.S.; Jiao, Z.; Getto, E.; Sun, K.; Monterrosa, A.M.; Maloy, S.A.; Anderoglu, O.; Sencer, B.H.; Hackett, M. Emulation of reactor irradiation damage using ion beams. *Scr. Mater.* **2014**, *88*, 33–36. [CrossRef]
9. Saidi, P.; Topping, M.; Dai, C.; Long, F.; Béland, L.K.; Daymond, M.R. The dependence of damage accumulation on irradiation dose rate in zirconium alloys: Rate theory, atomistic simulation and experimental validation. *J. Nucl. Mater.* **2021**, *543*, 152478. [CrossRef]
10. Was, G.S. The Damage Cascade. In *Fundamentals of Radiation Materials Science*; Springer: New York, NY, USA, 2017. [CrossRef]
11. Brailsford, A.D.; Bullough, R. The rate theory of swelling due to void growth in irradiated metals. *J. Nucl. Mater.* **1972**, *44*, 121–135. [CrossRef]

12. Mansur, L.K. Correlation of neutron and heavy-ion damage: II. The predicted temperature shift if swelling with changes in radiation dose rate. *J. Nucl. Mater.* **1978**, *78*, 156–160. [CrossRef]
13. Jin, P.; Shen, T.; Cui, M.; Zhu, Y.; Li, B.; Zhang, T.; Li, J.; Jin, S.; Lu, E.; Cao, X.; et al. Study on vacancy-type defects in SIMP steel induced by separate and sequential H and He ion implantation. *J. Nucl. Mater.* **2019**, *520*, 131–139. [CrossRef]
14. Zarkadoula, E.; Stoller, R.E. *Primary Radiation Damage Formation in Solids*; Oak Ridge National Lab.(ORNL): Oak Ridge, TN, USA, 2020.
15. Liu, H.; Huang, J.; Cao, L.; Su, Y.; Gao, Z.; Ma, P.; Xia, S.; Ge, W.; Liu, Q.; Zhao, S.; et al. Helium-hydrogen synergistic effects on swelling in in-situ multiple-ion beams irradiated steels. *Chin. Phys. B* **2021**, *30*, 086106. [CrossRef]
16. Clowers, L.N.; Jiao, Z.; Was, G.S. Synergies between H, He and radiation damage in dual and triple ion irradiation of candidate fusion blanket materials. *J. Nucl. Mater.* **2022**, *565*, 153722. [CrossRef]
17. Huang, J.; Liu, H.; Gao, Z.; Su, Y.; Liu, Q.; Ge, W.; Luo, F.; Xia, S.; Cao, L.; Xue, J.; et al. Helium-Hydrogen Synergistic Effects in Structural Materials Under Fusion Neutron Irradiation. *Front. Mater.* **2022**, *9*, 849115. [CrossRef]
18. Taller, S.; Was, G.S. Understanding bubble and void nucleation in dual ion irradiated T91 steel using single parameter experiments. *Acta Mater.* **2020**, *198*, 47–60. [CrossRef]
19. Katoh, Y.; Stoller, R.E.; Kohno, Y.; Kohyama, A. Numerical Estimation of Synergistic Effects of Displacement Damage and Helium Generation on Microstructural Evolution. *Mater. Trans. JIM* **1992**, *33*, 795–801. [CrossRef]
20. Katoh, Y.; Stoller, R.E.; Kohno, Y.; Kohyama, A. Modeling the effects of damage rate and He/dpa ratio on microstructural evolution. *J. Nucl. Mater.* **1992**, *191–194*, 1144–1149. [CrossRef]
21. Muroga, T.; Araki, K.; Yoshida, N.; Watanabe, H. Fission-fusion correlation of void swelling in pure nickel. *J. Nucl. Mater.* **1988**, *155–157*, 1290–1295. [CrossRef]
22. Budylkin, N.I.; Mironova, E.G.; Chernov, V.M.; Krasnoselov, V.A.; Porollo, S.I.; Garner, F.A. Neutron-induced swelling and embrittlement of pure iron and pure nickel irradiated in the BN-350 and BOR-60 fast reactors. *J. Nucl. Mater.* **2008**, *375*, 359–364. [CrossRef]
23. Huang, M.; Li, Y.; Ran, G.; Yang, Z.; Wang, P. Cr-coated Zr-4 alloy prepared by electroplating and its in situ He+ irradiation behavior. *J. Nucl. Mater.* **2020**, *538*, 152240. [CrossRef]
24. Kupriiyanova, Y.E.; Bryk, V.V.; Borodin, O.V.; Kalchenko, A.S.; Voyevodin, V.N.; Tolstolutskaya, G.D.; Garner, F.A. Use of double and triple-ion irradiation to study the influence of high levels of helium and hydrogen on void swelling of 8–12% Cr ferritic-martensitic steels. *J. Nucl. Mater.* **2016**, *468*, 264–273. [CrossRef]
25. Stoller, R.E.; Toloczko, M.B.; Was, G.S.; Certain, A.G.; Dwaraknath, S.; Garner, F.A. On the use of SRIM for computing radiation damage exposure. *Nucl. Instrum. Methods Phys. Res. Sect. B Beam Interact. Mater. At.* **2013**, *310*, 75–80. [CrossRef]
26. Zinkle, S.J.; Snead, L.L. Opportunities and limitations for ion beams in radiation effects studies: Bridging critical gaps between charged particle and neutron irradiations. *Scr. Mater.* **2018**, *143*, 154–160. [CrossRef]
27. Stevie, F.A.; Vartuli, C.B.; Giannuzzi, L.A.; Shofner, T.L.; Brown, S.R.; Rossie, B.; Hillion, F.; Mills, R.H.; Antonell, M.; Irwin, R.B.; et al. Application of focused ion beam lift-out specimen preparation to TEM, SEM, STEM, AES and SIMS analysis. *Surf. Interface Anal.* **2001**, *31*, 345–351. [CrossRef]
28. Agarwal, S.; Zinkle, S.J. Experimental Studies on Primary Damage Formation. In *Comprehensive Nuclear Materials*, 2nd ed.; Konings, R., Stoller, R., Eds.; Elsevier: Amsterdam, The Netherlands, 2020; Volume 1, pp. 74–90. [CrossRef]
29. Bacon, D.J.; Gao, F.; Osetsky, Y.N. The primary damage state in fcc, bcc and hcp metals as seen in molecular dynamics simulations. *J. Nucl. Mater.* **2000**, *276*, 1–12. [CrossRef]
30. Mansur, L.K. Theory and experimental background on dimensional changes in irradiated alloys. *J. Nucl. Mater.* **1994**, *216*, 97–123. [CrossRef]
31. Ge, W.; Zhao, S.; Wang, C.; Liu, H.; Su, Y.; Huang, J.; Gao, Z.; Xue, J.; Wang, Y. A Model for Dose Dependence of the Void Swelling in Electron-Irradiated Alloys. *Metals* **2022**, *12*, 244. [CrossRef]
32. Yang, X.; Deng, H.; Hu, N.; Xiao, S.; Ren, C.; Huai, P.; Wang, C.; Li, X.; Hu, W. Molecular Dynamics Simulation of the Displacement Cascades in Tungsten with Interstitial Helium Atoms. *Fusion Sci. Technol.* **2017**, *66*, 112–117. [CrossRef]
33. Qin, S.; Jin, S.; Niu, L.; Hao, J.; Zhou, H.; Lu, G. The effect of hydrogen on the recombination of Frenkel pair in tungsten: A theoretical insight. *Sci. China Phys. Mech. Astron.* **2017**, *60*, 067021. [CrossRef]
34. Hayward, E.; Deo, C. Synergistic effects in hydrogen-helium bubbles. *J. Phys. Condens. Matter* **2012**, *24*, 265402. [CrossRef]
35. Zimber, N.; Vladimirov, P.; Klimenkov, M.; Jäntsch, U.; Vila, R.; Chakin, V.; Mota, F. Microstructural evolution of three potential fusion candidate steels under ion-irradiation. *J. Nucl. Mater.* **2020**, *535*, 152160. [CrossRef]
36. Packan, N.H.; Farrell, K.; Stiegler, J.O. Correlation of neutron and heavy-ion damage. *J. Nucl. Mater.* **1978**, *78*, 143–155. [CrossRef]
37. Singh, B.N.; Zinkle, S.J. Defect accumulation in pure fcc metals in the trasient regime: A review. *J. Nucl. Mater.* **1993**, *206*, 212–229. [CrossRef]